

SUPPORTING INFORMATION

Deep defect level engineering: a strategy of optimizing the carrier concentration for high thermoelectric performance

Qian Zhang,^{a*} Qichen Song,^b Xinyu Wang,^a Jingying Sun,^c Qing Zhu,^c Keshab Dahal,^c Xi Lin,^a Feng Cao,^d Jiawei Zhou,^b Shuo Chen,^c Gang Chen,^b Jun Mao^{c*}, and Zhifeng Ren^{c*}

^aDepartment of Materials Science and Engineering, Harbin Institute of Technology, Shenzhen, Guangdong 518055, P.R. China, E-mail: zhangqf@hit.edu.cn

^bDepartment of Mechanical Engineering, Massachusetts Institute of Technology, Cambridge, Massachusetts 02139, USA

^cDepartment of Physics and TcSUH, University of Houston, Houston, Texas 77204, USA, E-mail: maojunte@gmail.com; zren@uh.edu

^dSchool of Science, Harbin Institute of Technology, Shenzhen, Guangdong 518055, P.R. China

Thermoelectric properties of I-doped PbTe

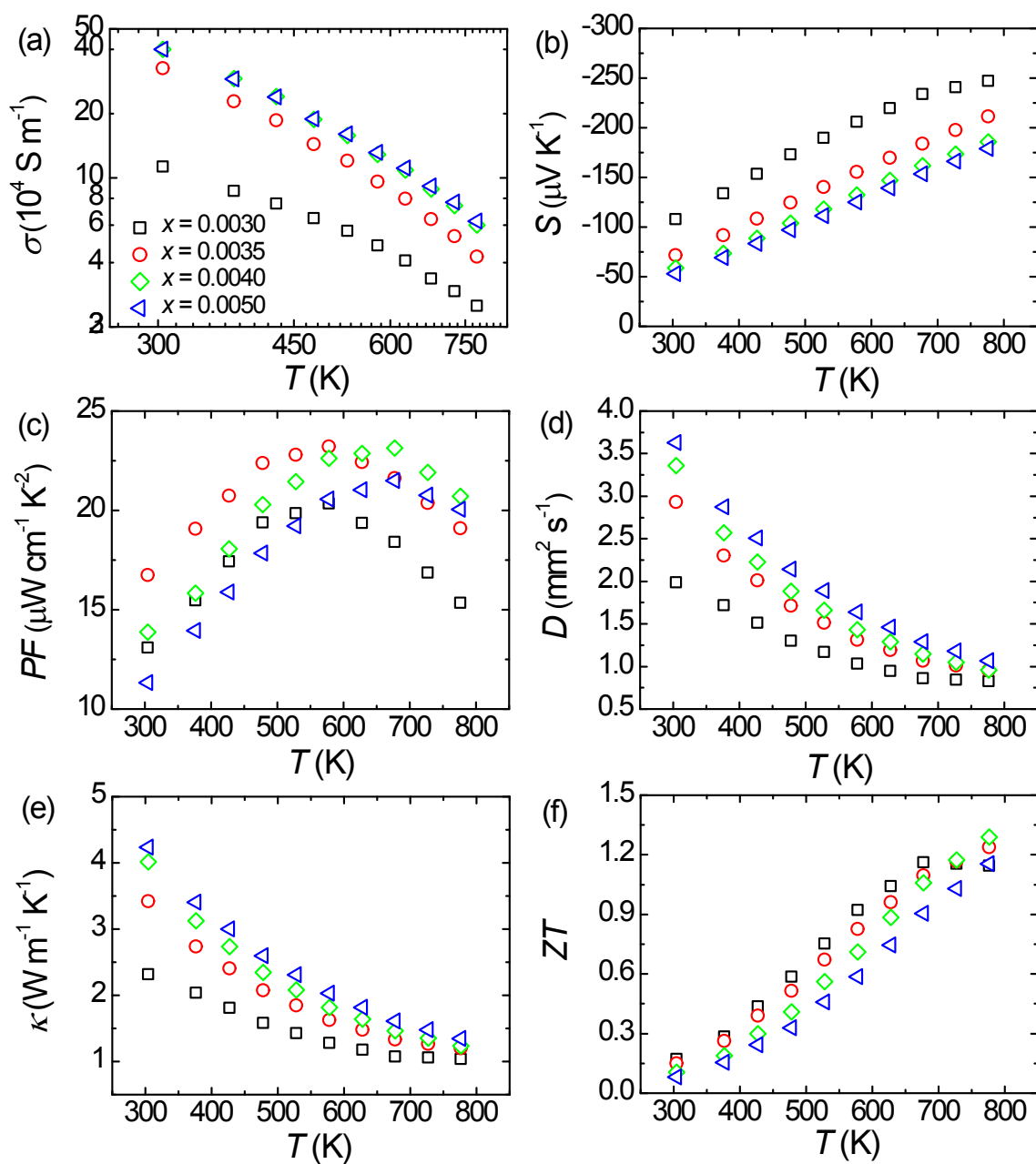


Figure S1. Thermoelectric properties of $\text{PbTe}_{1-x}\text{I}_x$ ($x = 0.003, 0.0035, 0.004, \text{ and } 0.005$). (a) Electrical conductivity, (b) Seebeck coefficient, (c) power factor, (d) thermal diffusivity, (e) thermal conductivity, and (f) ZT .

Pisarenko plot

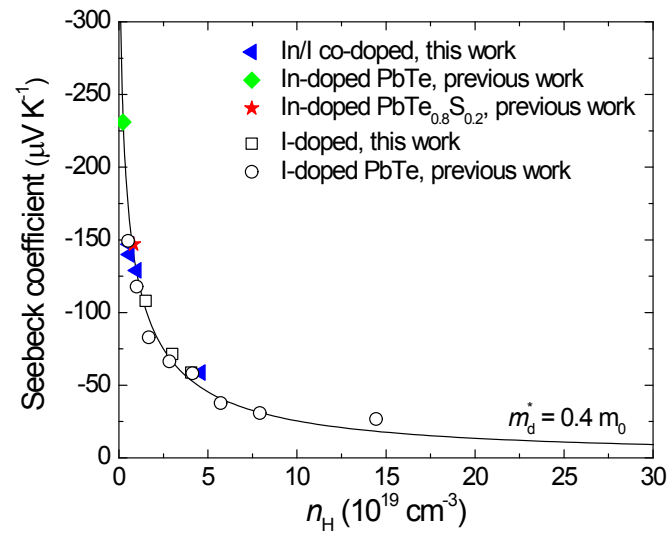


Figure S2. Pisarenko plot for the *n*-type PbTe-based materials.

Hall mobility

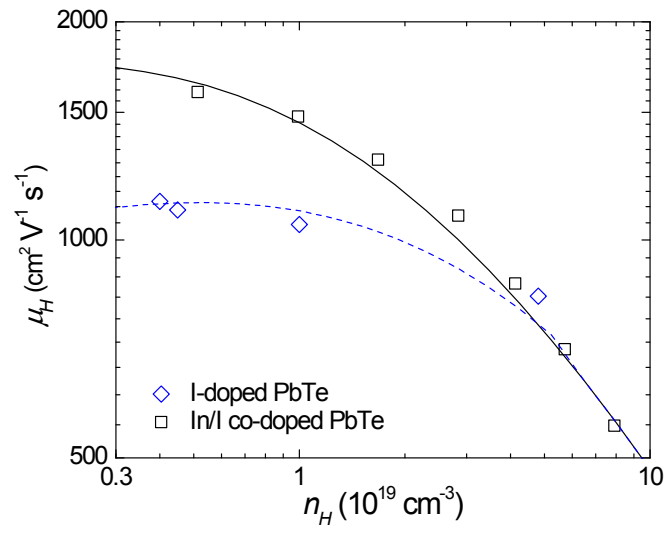


Figure S3. Relationship between the Hall carrier concentration and Hall carrier mobility of n -type PbTe.

Specific heat and diffusivity of In/I co-doped PbTe

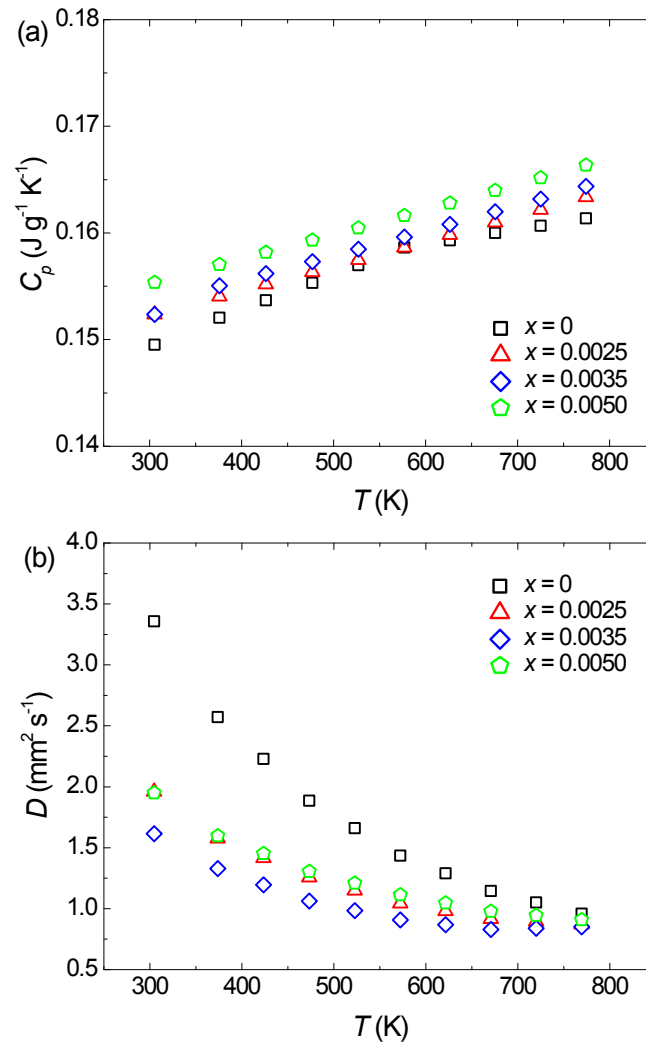


Figure S4. (a) Specific heat and (b) thermal diffusivity of In_xPb_{1-x}Te_{0.996}I_{0.004} ($x = 0, 0.0025, 0.0035,$ and 0.0050).

Lattice thermal conductivity of In/I co-doped PbTe

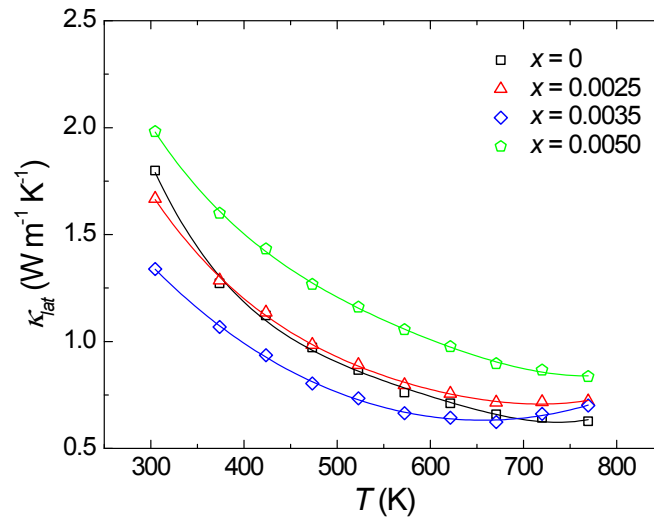


Figure S5. Temperature-dependent lattice thermal conductivity of In/I co-doped PbTe

The lattice thermal conductivity of the In/I co-doped PbTe is calculated as shown in Fig. S5. The lattice thermal conductivity shows a non-monotonic dependence on the indium concentration, which can be partially ascribed to the uncertainty in the estimation of the Lorenz number.

XRD

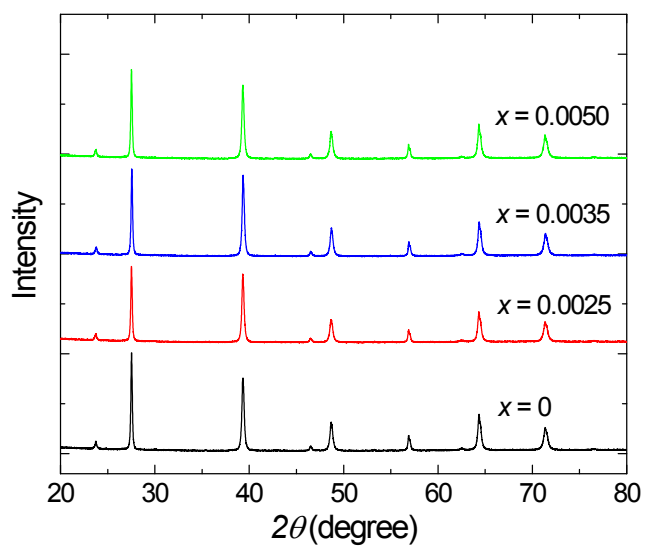


Figure S6. XRD patterns of $\text{PbTe}_{1-x}\text{I}_x$ ($x = 0.003, 0.0035, 0.004, \text{ and } 0.005$).

Details for calculation

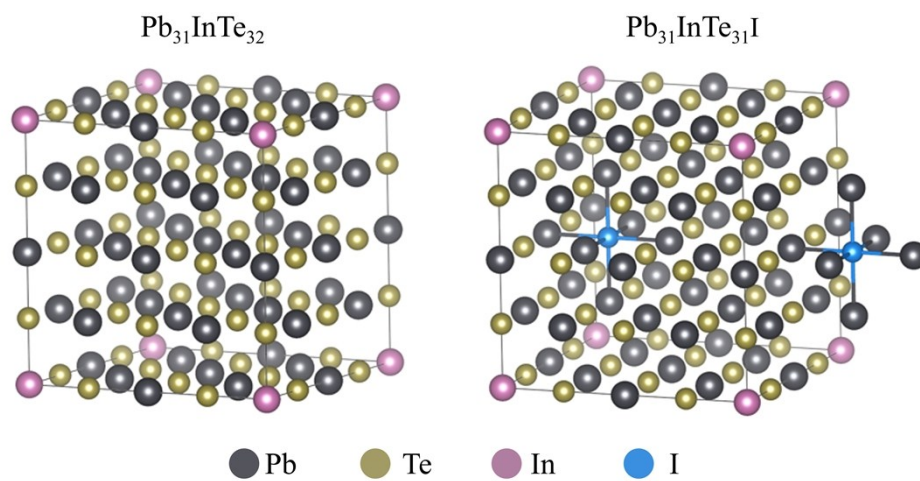


Figure S7. The structures of the supercell used in the calculation (a) $\text{Pb}_{31}\text{InTe}_{32}$, and (b) $\text{Pb}_{31}\text{InTe}_{31}\text{I}$